⌘ *Author's Choice*

THE JOURNAL OF BIOLOGICAL CHEMISTRY VOL. 284, NO. 41, pp. 28146–28155, October 9, 2009
© 2009 by The American Society for Biochemistry and Molecular Biology, Inc. Printed in the U.S.A.

Time-dependent Autoinactivation of Phospho-Thr^{286}-αCa^{2+}/Calmodulin-dependent Protein Kinase II*

Received for publication, April 8, 2009, and in revised form, July 22, 2009 Published, JBC Papers in Press, August 4, 2009, DOI 10.1074/jbc.M109.005900

Abdirahman M. Jama, Jon Fenton, Saralili D. Robertson, and Katalin Török[1]

From the Division of Basic Medical Sciences, St George's, University of London, Cranmer Terrace, London SW17 0RE, United Kingdom

Ca^{2+}/calmodulin-dependent protein kinase II (αCaMKII) is thought to exert its role in memory formation by autonomous Ca^{2+}-independent persistent activity conferred by Thr^{286} autophosphorylation, allowing the enzyme to remain active even when intracellular [Ca^{2+}] has returned to resting levels. Ca^{2+} sequestration-induced inhibition, caused by a burst of Thr$^{305/306}$ autophosphorylation via calmodulin (CaM) dissociation from the Thr$^{305/306}$ sites, is in conflict with this view. The processes of CaM binding, autophosphorylation, and inactivation are dissected to resolve this conflict. Upon Ca^{2+} withdrawal, CaM sequential domain dissociation is observed, starting with the rapid release of the first (presumed N-terminal) CaM lobe, thought to be bound at the Thr$^{305/306}$ sites. The time courses of Thr$^{305/306}$ autophosphorylation and inactivation, however, correlate with the slow dissociation of the second (presumed C-terminal) CaM lobe. Exposure of the Thr$^{305/306}$ sites is thus not sufficient for their autophosphorylation. Moreover, Thr$^{305/306}$ autophosphorylation and autoinactivation are shown to occur in the continuous presence of Ca^{2+} and bound Ca^{2+}/CaM by time courses similar to those seen following Ca^{2+} sequestration. Our investigation of the activity and mechanisms of phospho-Thr$_{286}$-αCaMKII thus shows time-dependent autoinactivation, irrespective of the continued presence of Ca^{2+} and CaM, allowing a very short, if any, time window for Ca^{2+}/CaM-free phospho-Thr^{286}-αCaMKII activity. Physiologically, the time-dependent autoinactivation mechanisms of phospho-Thr^{286}-αCaMKII ($t_{1/2}$ of ~50 s at 37 °C) suggest a transient kinase activity of ~1 min duration in the induction of long term potentiation and thus memory formation.

Ca^{2+}/calmodulin-dependent protein kinase II (αCaMKII)[2] is essential in hippocampal learning and *N*-methyl-D-aspartate receptor-dependent synaptic plasticity, causing long term potentiation (1, 2). The exact mechanisms of αCaMKII in memory functions have not yet been identified.

αCaMKII is a broad specificity Ser/Thr protein kinase, which catalyzes the phosphorylation of over 100 protein and peptide substrates *in vitro* (3). Uniquely, the CaMKII family possesses two distinct kinase mechanisms. The first mechanism is a "canonical" intrasubunit phosphorylation, commonly found in monomeric kinases, in which the phosphorylatable residue of the substrate bound to the helical subdomain of the catalytic domain at the active site is lined up with the terminal phosphate of ATP (4). Although there is a large number of potential "canonical" substrates for αCaMKII at the synapse (5), so far AMPA receptors have been shown to be possible physiological substrates of αCaMKII (6). For the purpose of this study, syntide 2, a commonly used peptide substrate derived from phosphorylation site 2 of glycogen synthase (7), was chosen.

The second mechanism, intersubunit autophosphorylation, takes advantage of the oligomeric organization of CaMKII (8). The most important autophosphorylation site in the α isoform is Thr^{286}, which resides in the vicinity of the autoinhibitory domain (9). Peptide substrates with homologous sequences to this region have been reported to be phosphorylated by αCaMKII. This, however, occurs with a low V_{max}, and these substrates show properties of a non-competitive inhibitor with respect to phosphorylation of "canonical" substrates (10) and of Thr^{286} autophosphorylation itself (11). Examples of such substrates include autocamtide, a peptide substrate derived from the autoinhibitory region (12) and the NR2B subunit of the *N*-methyl-D-aspartate receptor, which has been identified as a potential physiological target of phospho-Thr^{286}-αCaMKII at the postsynaptic membrane (13). The possible physiological significance of NR2B phosphorylation is not yet known. There is evidence to suggest that Thr^{286} autophosphorylation is required to achieve full activity of the enzyme, since the unphosphorylatable T286A mutant enzyme has much diminished activity compared with wild type enzyme (14, 15).

Thr^{286} autophosphorylation causes CaM "trapping," a >10^4-fold increase in the affinity of αCaMKII for Ca^{2+}/CaM (16–18). At the same time, Thr^{286} autophosphorylation is also attributed to confer Ca^{2+}- and CaM-independent persistent "autonomous" kinase activity to αCaMKII. However, due to the extremely high affinity of phospho-Thr$_{286}$-αCaMKII for Ca^{2+}/CaM, [Ca^{2+}] of <10 nM is required to achieve full dissociation of Ca^{2+}/CaM, since CaM trapping occurs by virtue of Ca^{2+} trapping (19). Partial activity measured upon partial Ca^{2+} withdrawal therefore may not always reflect Ca^{2+}/CaM-free enzyme (9). Furthermore, the physiological resting [Ca^{2+}] range is 50–100 nM; therefore, phospho-Thr^{286}-αCaMKII is

* This work was supported by Wellcome Trust Project Grant 075931 (to K. T.).
⌘ *Author's Choice*—Final version full access.
[1] To whom correspondence should be addressed. Tel.: 442087255832; Fax: 442087253581; E-mail: k.torok@sgul.ac.uk.
[2] The abbreviations used are: αCaMKII, Ca^{2+}/calmodulin-dependent protein kinase II; AEDANS, 5-(2-acetylamino)-ethylamino-naphtalene-1-sulfonic acid; AMPA, α-amino-3-hydroxyl-5-methyl-4-isoxazole-propionate; CaM, calmodulin; CaMKIV, Ca^{2+}/calmodulin-dependent protein kinase IV; DA-CaM, AEDANS/DDP-T34C/T110C-calmodulin; DDP, *N*-(4-dimethylamino-3,5-dinitrophenyl); E_a, activation energy; FL, *5*-(4,6-dichlorotriazinyl)aminofluorescein; NR2B, subunit 2B of *N*-methyl-D-aspartate receptor; PIPES, piperazine-*N*,*N*′-bis-(2-ethanesulfonic acid).

likely always to have residual Ca^{2+}/CaM bound. This may be partially Ca^{2+}-saturated CaM (19).

Persistent autonomous activity conferred by Thr^{286} autophosphorylation is thought to enable αCaMKII to function as a memory molecule (20, 21). In contrast, however, following the development of chemical long term potentiation, rapid inactivation has also been reported (22). The extent of an autonomous activity is further obscured by the finding that Ca^{2+} sequestration induces a burst of autophosphorylation at residues $Thr^{305/306}$, followed by a loss of activity (23). Moreover, when examined across a broad range of $[Ca^{2+}]$, the Ca^{2+}/CaM dependence of phospho-Thr^{286}-αCaMKII activity is apparent (19). It is thus vital to establish the mechanisms of activation and inactivation of αCaMKII at the molecular level in order to understand how it may function physiologically in learning and memory. To this end, it is necessary to dissect the mechanisms of Ca^{2+}/CaM dissociation, $Thr^{305/306}$ autophosphorylation, and inactivation of phospho-Thr^{286}-αCaMKII and to establish the time window for autonomous Ca^{2+}/CaM-independent activity.

MATERIALS AND METHODS

Proteins—Mouse αCaMKII (cDNA kindly provided by Dr. D. Brickey and Prof. T. R. Soderling, Vollum Institute, Oregon Health and Science University, Portland, OR) was overexpressed in baculovirus-transfected Sf9 insect cells and purified by CaM-Sepharose and Mono Q fast protein liquid chromatography (17). Rat CaMKIV (cDNA kindly provided by Dr. K. A. Anderson and Prof. A. R. Means, Department of Pharmacology and Cancer Biology, Duke University Medical Center, Durham, NC) was purified by the same method. Human liver recombinant calmodulin, Lys^{75}-FL-calmodulin (FL-CaM), and AEDANS/DDP-T34C/T110C-CaM (DA-CaM) were generated as described previously (17, 24). Mouse monoclonal anti-phospho-Thr^{286}- and rabbit polyclonal anti-phospho-Thr^{305}-αCaMKII antibodies were purchased from Millpore Chemicon. Western blotting was carried out as previously described, and antibodies were used at a 1:1000 dilution (19).

Protein Concentration Measurements—Protein concentrations were determined spectrophotometrically using molar extinction coefficients (ϵ_o) calculated from the amino acid composition: αCaMKII (subunits), $\epsilon_o = 64{,}805\ M^{-1}\ cm^{-1}$ (280 nm); CaM, $\epsilon_o = 3{,}300\ M^{-1}\ cm^{-1}$ (278 nm); CaMKIV, $\epsilon_o = 47{,}330\ M^{-1}\ cm^{-1}$ (280 nm) (17). The concentration of FL-CaM was determined using $\epsilon_o = 70{,}000\ M^{-1}\ cm^{-1}$ (492 nm) at pH 9.0 (Molecular Probes).

Time Course of Thr^{286} and $Thr^{305/306}$ Autophosphorylation of αCaMKII—6 μM αCaMKII, 8 μM calmodulin, and 1 mM ATP were incubated in 50 mM K^+-PIPES, pH 7.0, 100 mM KCl, 2 mM $MgCl_2$, 5 mM 1,4-dithiothreitol, and 0.05 mM $CaCl_2$ at 21, 30, and 37 °C for various times from 0 to 3600 s. The reaction was either allowed to proceed in the presence of Ca^{2+}, or 4.2 mM EGTA was added at 15 s, and the reaction was terminated using 4× SDS sample buffer at predefined time points. The phospho-Thr^{286}-αCaMKII was detected by Western blotting using a specific mouse monoclonal anti-phospho-Thr^{286}-αCaMKII and anti-phospho-$Thr^{305/306}$-αCaMKII antibodies as described in Ref. 19. The time course was assessed by densitometry of Western blots using a Fuji Film Luminescent Image Analyzer with LAS4000IR software. Densitometry was carried out using ImageJ software from the National Institutes of Health as follows. The average density reading for each band on the Western blot and a reading for the background was taken. The following formula was used to calculate relative density on an inverted scale: $(D_{max} - D_t)/(D_{max} - D_B)$, where D_{max} represents the average density of the darkest band, D_t is the average density at a particular time point, and D_B is the average density of the background. The scale was thus inverted by subtracting each value from the highest density value. Relative density was calculated with reference to the highest density, and the data were fitted with an exponential function using the GraFit software program, version 4.0.

Steady-state Assay of αCaMKII Enzyme Activity—A continuous enzyme-linked spectrofluorometric assay was used to determine ADP production by monitoring the decrease in NADH fluorescence due to its oxidation to NAD^+. Fluorescence excitation was set to 340 nm, and emission was detected at 460 nm. The experiments were carried out at the specified temperatures. Typically, 5 mM 1,4-dithiothreitol, 4.5 units of lactate dehydrogenase, 2 units of pyruvate kinase, 2 mM phosphoenolpyruvate, 22 μM NADH, 6 μM calmodulin, 50 μM syntide-2, and 1 mM ATP were present in the assay mix. 0.1 μM αCaMKII or phospho-Thr^{286}-αCaMKII was added last to a final volume of 0.05 ml of assay solution (19).

Free Ca^{2+} concentrations of Ca^{2+}/EGTA mixtures were calculated using a K_d value of 4.35×10^{-7} M, which was determined in buffer conditions and ionic strength similar to those used in this study (25). A Fortran program was written to solve the quadratic equation, $[Ca^{2+}] = (b \pm \sqrt{(b^2 - 4x\,[Ca^{2+}]_o \times [EGTA]_o)})/2$, where $b = K_d + [Ca^{2+}]_o + [EGTA]_o$ from total Ca^{2+} $[Ca^{2+}]_o$, total EGTA $[EGTA]_o$, and the K_d. To verify the calculated $[Ca^{2+}]$ concentrations, the fluorescent Ca^{2+} indicator fluo3 was titrated in Ca^{2+}/EGTA mixtures. Best fit to the titration curve gave a K_d value of 433 ± 55 nM for fluo3, in good agreement with the K_d value of 390 nM previously described for fluo3 (Molecular Probes), thus verifying our calculated $[Ca^{2+}]$ values (19).

Fluorescence Spectroscopy—Stopped-flow kinetic measurement of DA-CaM dissociation was carried out using a Hi-Tech Scientific SF-61DX2 stopped-flow system as follows. Fluorescence excitation was set to 365 nm with a 1-nm slit width, and fluorescence emission from AEDANS was collected using a 400 nm cut-off filter. The assay solution contained 50 mM K^+-PIPES, pH 7.0, 100 mM KCl, 2 mM $MgCl_2$. Equilibrium fluorescence measurements of DA-CaM and FL-CaM polarization were carried out using a SLM Model 8000 spectrofluorimeter by ISS, Inc. (champaign, IL).

Software—Data were analyzed using the GraFit software program, version 4.0. Stopped-flow kinetic data were fitted using the KinetAsyst software program (Hi-Tech Scientific).

RESULTS

Thr^{286} Autophosphorylation in the Presence of an Exogenous "S" Type Peptide Substrate—Thr^{286} autophosphorylation is a rapid reaction that occurs immediately upon Ca^{2+}/CaM and

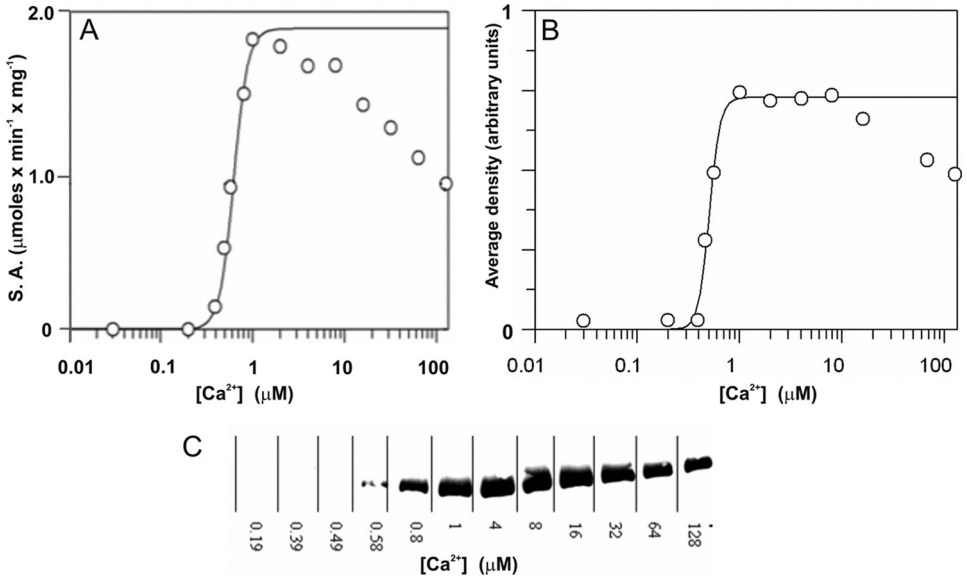

FIGURE 1. **Ca^{2+} dependence of peptide substrate and Thr^{286} autophosphorylation by αCaMKII.** *A*, steady-state activity of 50 nM enzyme in the presence of 50 μM syntide 2 as peptide substrate was measured at 25 °C at the indicated Ca^{2+} concentrations. *B*, Thr^{286} autophosphorylation was quantified by densitometry of Western blots as shown in *C*. A mouse monoclonal anti-phospho-αCaMKII (Thr^{286}) antibody was used (Millipore). *C*, autophosphorylation mixtures containing 6 μM αCaMKII, 8 μM CaM, 50 μM syntide 2, and 1 mM ATP at the specified [Ca^{2+}] were incubated for 15 s at 25 °C, and the reaction was quenched with SDS sample buffer. Western blot of samples is shown.

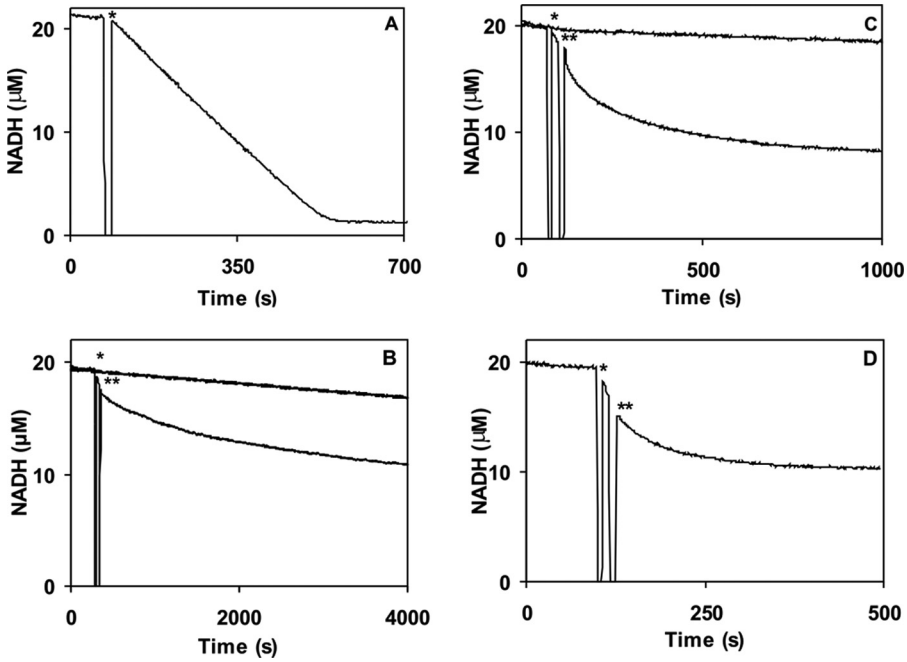

FIGURE 2. **Temperature-dependent αCaMKII activity and Ca^{2+} sequestration-induced inactivation of Ca^{2+}/CaM·phospho-Thr^{286}-αCaMKII.** *A*, steady-state activity measured by an NADH-coupled assay as described under "Materials and Methods." 50 nM αCaMKII was added (indicated by the *asterisk*) to start the reaction in the presence of 50 μM syntide 2 as peptide substrate at 10 μM [Ca^{2+}] concentration at 21 °C. Temperature-dependent steady-state activity and inactivation induced by the addition of 4.2 mM EGTA at 21 °C (*B*), 30 °C (*C*), and 37 °C (*D*) were measured. The reaction was started by the addition of the enzyme, marked by an *asterisk*. A *double asterisk* denotes where 4.2 mM EGTA was added. As a base-line control, NADH fluorescence was monitored prior to starting the reaction by the addition of the enzyme (the section before that marked with an *asterisk*). In *B* and *C*, which had the longest time courses, additionally independent photobleaching controls were also run for the same duration as the experiment (*top lines*). The fluorescence decay rates due to enzyme activity or inactivation by EGTA were corrected for the appropriate base line.

ATP activation of αCaMKII and changes the enzyme properties (19). It was therefore important to know whether αCaMKII in our steady-state assays was Thr^{286}-phosphorylated. To determine the state of αCaMKII with regard to Thr^{286} autophosphorylation, first the Ca^{2+} dependence of phosphorylation of exogenous peptide substrate syntide 2 was compared with that of Thr^{286} autophosphorylation. The Ca^{2+} dependence of phosphorylation of peptide substrate syntide 2, shown in Fig. 1*A*, revealed a K_m of 612 ± 26 nM for Ca^{2+}, a V_{max} of 2.0 ± 0.2 μmol × min^{-1} × mg of enzyme, and a Hill coefficient (*n*) of 5.6 ± 0.5 at 25 °C. The K_m and *n* values were similar to those previously determined for the Ca^{2+} dependence of αCaMKII activation of phosphorylation of protein substrate smooth muscle myosin light chain kinase, whereas the V_{max} for syntide 2 was higher than that for smooth muscle myosin light chain kinase (19).

Thr^{286} autophosphorylation of αCaMKII in the presence of saturating peptide substrate syntide 2 was analyzed by Western blotting. As shown in Fig. 1, *B* and *C*, a K_m of 500 ± 14 nM for Ca^{2+} and an *n* value of 8.2 ± 1.7 for Thr^{286} autophosphorylation were measured. These data showed that exogenous substrate phosphorylation and Thr^{286} autophosphorylation by αCaMKII were activated in the same [Ca^{2+}] concentration range and that saturating exogenous peptide substrate did not effectively compete with Thr^{286} autophosphorylation. These data support the existence of distinct phosphorylation mechanisms at the "canonical" and the Thr^{286} site with a low level of competition presented by "canonical" phosphorylation to Thr^{286} autophosphorylation.

Ca^{2+} Sequestration-induced Inactivation of Ca^{2+}/CaM·Phospho-Thr^{286}-αCaMKII—Following activation and thus Thr^{286} autophosphorylation, EGTA is thought to expose "autonomous" activity of αCaMKII (9), but the enzyme is also reported to undergo a burst of inhibitory $Thr^{305/306}$ autophosphorylation (7). In order to dissect this process, first the time course of kinase activity during syntide 2 phosphorylation activity was monitored. As shown in Fig. 2, *A–D*, steady-state activity was initiated by the addition of

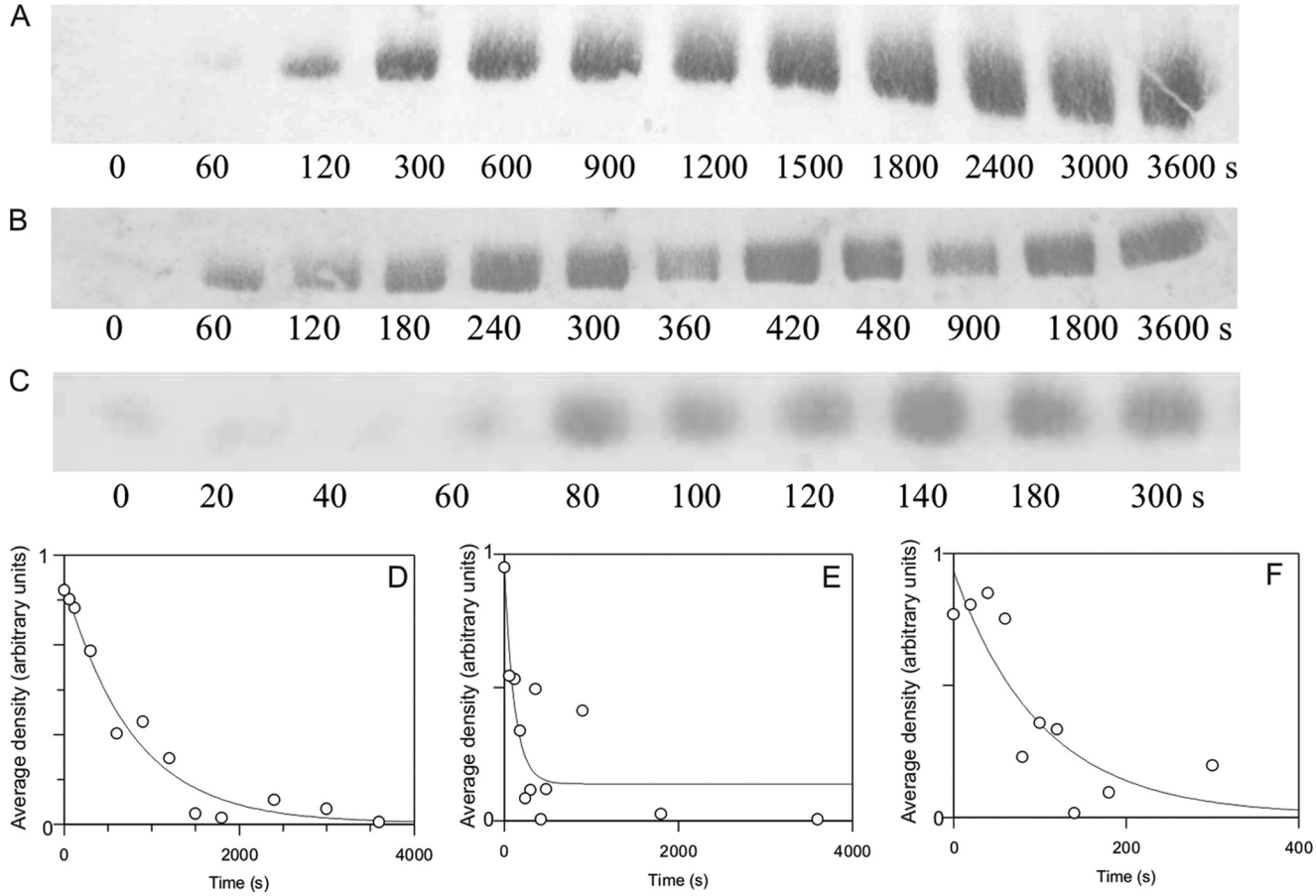

FIGURE 3. **Thr$^{305/306}$ autophosphorylation time course estimated by Western blotting.** 1 μM αCaMKII was allowed to autophosphorylate for 15 s, as described under "Materials and Methods." At that point, 4.2 mM EGTA was added, and aliquots were taken at the indicated time points; the reaction was quenched by pipetting the aliquots taken into SDS sample buffer. A rabbit polyclonal anti-phospho-αCaMKII (Thr^{305}) (Millipore) was used. Shown are Western blots and respective densitometric analyses of representative time courses at 21 (*A* and *D*), 30 (*B* and *E*), and 37 °C (*C* and *F*). Densitometric analysis of Western blots was carried out as described under "Materials and Methods."

αCaMKII into the assay as denoted by the *asterisks*. At the points indicated by *double asterisks*, 4.2 mM EGTA was added, and this induced an exponential decay of activity. The rate constants of EGTA-induced inactivation were 0.0017 s^{-1}, 0.0053 s^{-1}, and 0.0125 s^{-1} at 21, 30, and 37 °C, respectively. In order to exclude the possibility that inactivation occurred due to unfolding, Trp fluorescence, an indicator of the integrity of the tertiary structure of proteins, of αCaMKII in the assay conditions was monitored. EGTA caused a rapid quenching of Trp fluorescence; there were, however, no further changes in the slow time course of inactivation (data not shown). The EGTA-induced autoinactivation time courses were next compared with those of Thr$^{305/306}$ autophosphorylation, the dissociation of Ca^{2+}, and the subsequent release of CaM from the Ca^{2+}/CaM·phospho-Thr^{286}-αCaMKII complex.

Time Course of Thr$^{305/306}$ Autophosphorylation Induced by Ca^{2+} Sequestration—The rate of Thr$^{305/306}$ autophosphorylation of Ca^{2+}/CaM·phospho-Thr^{286}-αCaMKII induced by EGTA was estimated from the semiquantitative densitometric analysis of Western blots (Fig. 3, *A–C*). Rate constants of 0.0013 s^{-1} at 21 °C, 0.0086 s^{-1} at 30 °C, and 0.0098 s^{-1} at 37 °C were obtained (see Table 1). The EGTA-induced Thr$^{305/306}$ autophosphorylation and autoinactivation rates (shown above; Fig. 2) were thus closely related.

Mechanism of CaM Dissociation in Ca^{2+} Sequestration-induced Autoinactivation of Phospho-Thr^{286}-αCaMKII—The kinetics of Ca^{2+} dissociation from Ca^{2+}/CaM·phospho-Thr^{286}-αCaMKII had previously been examined. Ca^{2+} dissociation rate constants were 8 s^{-1} for one site, 0.31 s^{-1} for two of the sites, and 0.023 s^{-1} for the one remaining site at 21 °C (19).

To study CaM dissociation kinetics, DA-CaM, a probe of CaM conformation with the fluorescent donor quenching reporting distance changes between the N and C lobes of CaM (17), was used. Conformational changes of CaM were monitored during the time course of inactivation of phospho-Thr$_{286}$-αCaMKII upon the addition of EGTA. Stopped-flow kinetic experiments in which αCaMKII, DA-CaM, and ATP premixed in the presence of Ca^{2+} were rapidly reacted with 25 mM EGTA showed a biphasic process; DA-CaM became extended with two rate constants: 0.82 s^{-1} (amplitude 0.70) and 0.088 s^{-1} (amplitude 0.30) at 21 °C (Fig. 4*A* and Table 1).

These data showed that both Ca^{2+} dissociation and CaM "stretching" were more rapid than Thr$^{305/306}$ autophosphorylation and inactivation (Table 1). However, DA-CaM unquenching may not have signified its complete dissociation, and instead it may have indicated that DA-CaM adopted an extended conformation as a result of the dissociation of one of its lobes only (17); thus, fluorescence polar-

TABLE 1

Inactivation and dissociation rates of the Ca^{2+}/αCaM·phospho-Thr^{286}-CaMKII complex

The autoinactivation processes of the Ca^{2+}/CaM·phospho-Thr^{286}-αCaMKII complex were dissected by measurements of Ca^{2+} and CaM dissociation, inactivation, and Thr^{305} autophosphorylation rates.

Temperature	*k*						
	Ca^{2+} off[a]	CaM "stretching"	CaM dissociation (polarization) (slow phase)	Inhibition (EGTA)	Thr^{305} autophosphorylation (EGTA)	Inhibition (Ca^{2+})	Thr^{305} autophosphorylation (Ca^{2+})
				s^{-1}			
21 °C	8 ± 1.4			0.00105 ± 0.00047 (n = 4)[c]	0.0013 ± 0.0002	0.000450 ± 0.000002[d] (n = 2)[c]	0.0013 ± 0.0002
	0.31 ± 0.03	0.82 ± 0.02 (0.70)[b]					
	0.023 ± 0.016	0.088 ± 0.002 (0.30)[b]					
30 °C				0.00485 ± 0.00064 (n = 2)[c]	0.0086 ± 0.0002	0.0043 ± 0.0028 (n = 3)[c]	0.0060 ± 0.0051 (n = 2)[c]
37 °C			0.0200 ± 0.0075[e] (n = 5)[c]	0.01255 ± 0.00007 (n = 2)[c]	0.0098 ± 0.0064	0.01335 ± 0.00092 (n = 2)[c]	0.0157 ± 0.0050

[a] Data from Tzortzopoulos *et al.* (19).
[b] Relative amplitude.
[c] n specifies the number of independent experiments; the mean and the S.D. are shown. Where n = 1, the fitted value and the S.E. of the fit is given.
[d] The temperature in this experiment was 22 °C.
[e] A p value of 0.244 obtained using an unpaired two-tailed t test showed this value not to be significantly different from the rate constant of 0.01255 ± 0.000071 (S.D.) s^{-1} (n = 2) obtained for inhibition induced by EGTA.

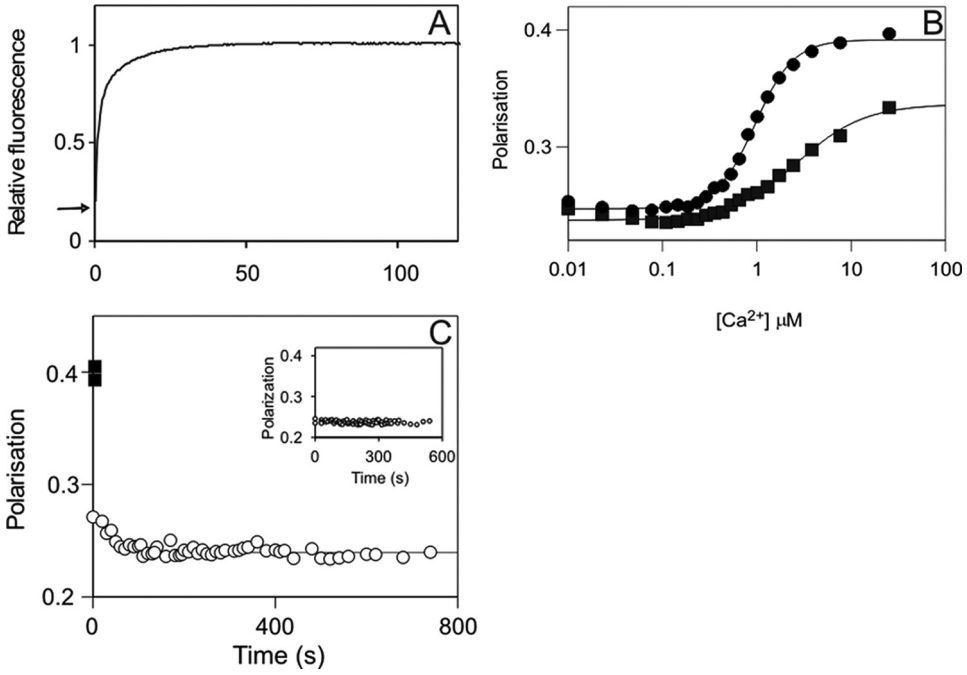

FIGURE 4. **Mechanism of CaM dissociation from its complex with phospho-Thr^{286}-αCaMKII upon Ca^{2+} sequestration.** *A*, calmodulin stretching shown by DA-CaM unquenching. The mixture of 1 μM αCaMKII, 1 μM DA-CaM, and 0.5 mM ATP in 50 mM K-PIPES, pH 7.0, 100 mM KCl, 2 mM $MgCl_2$, 1 mM 1,4-dithiothreitol, and 0.1 mM $CaCl_2$ was rapidly mixed with 50 mM EGTA adjusted to pH 7.0 with KOH at 21 °C. DA-CaM fluorescence (donor AEDANS was excited at 365 nm, and emission was detected using a 455 nm cut-off filter) was quenched in complex with phospho-Thr_{286}-αCaMKII. The *arrow* indicates relative fluorescence 0.2. Upon EGTA addition, DA-CaM fluorescence was unquenched in a biphasic process. *B*, polarization of FL-CaM upon Ca^{2+}-dependent binding to αCaMKII (*squares*) and CaMKIV (*diamonds*). The mixture of 120 nM FL-CaM and 1.4 μM CaMKIV or 2.0 μM αCaMKII in the same conditions as above except for the presence of 2 mM EGTA was titrated with $CaCl_2$. [Ca^{2+}] was determined as described under "Materials and Methods" (19). *C*, FL-CaM dissociation from phospho-Thr^{286}-αCaMKII was monitored by polarization. ■, the starting values of polarization of the Ca^{2+}/FL-CaM·phospho-Thr^{286}-αCaMKII; the time course of polarization decay (○) upon the addition of 4.2 mM EGTA is shown. *Inset*, controls that contained no ATP but in which 2 mM EGTA was present from the start (n = 4); these show no time-dependent change. In the *main panel*, a mean rate constant of 0.0200 ± 0.0075 s^{-1} (±S.D.) was obtained for the polarization data on CaM dissociation (n = 5).

ization was used to further probe the state of CaM binding to phospho-Thr^{286}-αCaMKII.

Ca^{2+} Sequestration-induced FL-CaM Dissociation Monitored by Polarization—Steady-state polarization measurements showed that FL-CaM (24) was a useful probe of CaM binding to protein kinases αCaMKII and CaMKIV. As seen in Fig. 4*B*, FL-CaM polarization increased from 0.24 to 0.4 and 0.33 upon Ca^{2+}-dependent association with CaMKIV and αCaMKII, respectively, in the absence of ATP or protein substrates in the [Ca^{2+}] range applied. The high polarization of Ca^{2+}/CaM in complex with CaMKIV (*P*, 0.39) was consistent with compact Ca^{2+}/CaM binding to CaMKIV indicating that both CaM lobes were engaged[3]; similarly, the lower polarization of Ca^{2+}/CaM in complex with unphosphorylated αCaMKII in the absence of ATP and protein substrates (*P*, 0.34) was consistent with Ca^{2+}/CaM binding in an extended conformation, mainly with one lobe only (17). The differences in affinities governed by the binding conformations were also in accord with a greater effect on the Ca^{2+} binding affinities in the Ca^{2+}/CaM·CaMKIV complex (K_d for Ca^{2+}, 0.96 ± 0.03 μM) compared with that in the Ca^{2+}/CaM·αCaMKII complex (K_d for Ca^{2+}, 2.70 ± 0.37 μM). The lack of involvement of both lobes of CaM in binding to αCaMKII was also reflected in a low Hill coefficient, n = 1.22 ± 0.14 in contrast with n = 2.13 ± 0.10 for CaMKIV.

In order to probe the dissociation process of CaM by polarization, Ca^{2+}/CaM·phospho-Thr^{286}-αCaMKII was generated

[3] K. Török, unpublished data.

in a mixture of αCaMKII with Ca^{2+}/FL-CaM and ATP; this resulted in an increase of polarization from 0.23 to 0.4 consistent with high affinity compact binding of Ca^{2+}/CaM (17). Upon the addition of EGTA, most of the polarization was rapidly reversed, reaching 0.27 after 15 s, indicating that CaM became substantially more flexible than it was in the presence of Ca^{2+}; this was most likely due to the dissociation of one of its lobes. The rapid phase of depolarization was, however, followed by a slow phase with a rate constant of 0.0200 s^{-1} at 37 °C (Fig. 4*C*). The EGTA-induced inactivation rate constant was 0.0125 s^{-1} at the same temperature. There was no significant difference between the two values (Fig. 4*C* and Table 1).

Temperature Dependence of Autoinactivation of Phospho-Thr^{286}-αCaMKII in the Presence of Ca^{2+}—A burst of autoinhibition triggered by the addition of EGTA has been well documented (7). We have, however, previously also observed a loss of activity upon incubating αCaMKII in the presence of Ca^{2+}, CaM, ATP at 30 °C for 2 min[4] and have decided to further investigate the phenomenon. From the data shown in Fig. 1, it is evident that the enzyme complex that undergoes this inactivation is Ca^{2+}/CaM·phospho-Thr^{286}-αCaMKII. First, autoinactivation of Ca^{2+}/CaM·phospho-Thr^{286}-αCaMKII was measured in the presence of peptide substrate syntide 2. Fig. 5, *A–C*, shows the time courses of activity in the presence of syntide 2 and an ATP-regenerating system at 22, 30, and 37 °C. It can be seen that αCaMKII activity was lost in an exponential process, and the rate constants of Ca^{2+}-dependent autoinactivation were 0.0004 s^{-1} at 22 °C, 0.0043 s^{-1} at 30 °C, and 0.0127 s^{-1} at 37 °C, similar to those obtained by inactivation in EGTA (Table 1).

Thr$^{305/306}$ Autophosphorylation in the Presence of Ca^{2+}—We then asked if Thr$^{305/306}$ autophosphorylation occurred in the presence of Ca^{2+}. As seen in Fig. 6, *A–C*, Thr$^{305/306}$ autophosphorylation occurred in these conditions. At 50 μM Ca^{2+}, the rate constants for Thr$^{305/306}$ autophosphorylation were estimated from densitometric analysis of Western blots as 0.0013 s^{-1} at 21 °C, 0.0024 s^{-1} at 30 °C, and 0.0157 s^{-1} at 37 °C (Fig. 6, *D–F*). These values were not significantly different from those seen when Thr$^{305/306}$ autophosphorylation was thought to be induced by Ca^{2+} removal by the addition of 4.2 mM EGTA. These data also highlight that autoinactivation of Ca^{2+}/CaM·phospho-Thr^{286}-αCaMKII in the presence and, as described above, in the absence of Ca^{2+} has a physiologically relevant time course, with a half-life of ~50 s at 37 °C.

CaM Conformation during Autoinactivation of αCaMKII in Ca^{2+}—We have shown above that αCaMKII becomes inactivated upon continued incubation with Ca^{2+}/CaM and ATP following its activation. Thr$^{305/306}$ autophosphorylation was also detected during the period of inactivation. Since the Thr$^{305/306}$ sites are located in the CaM binding domain, it was expected that Ca^{2+}/CaM may be displaced by Thr$^{305/306}$ autophosphorylation. We thus checked if Ca^{2+}/CaM remained bound or dissociated during inactivation, using DA-CaM (see above). The fluorescence of DA-CaM is strongly quenched when bound to a target in a compact conformation, due to the donor and acceptor labels on the N and C lobes of CaM being in a closer proximity than the critical distance between them for resonance energy transfer. Unbound CaM is more extended, and less energy transfer is shown by the greater, unquenched fluorescence. A complex of Ca^{2+}/DA-CaM·αCaMKII also has high fluorescence (relative fluorescence 1), since CaM is bound in an extended conformation (17). Fig. 7 shows that upon the addition of ATP, which results in immediate Thr^{286} autophosphorylation and Ca^{2+}/CaM trapping, the fluorescence of DA-CaM becomes quenched, indicating that Ca^{2+}/DA-CaM is bound in a compact conformation. It was expected that at least one CaM lobe, assumed to be the N lobe covering the Thr$^{305/306}$ sites, dissociates, allowing CaM to adopt the extended conformation during Thr$^{305/306}$ autophosphorylation. It is clearly

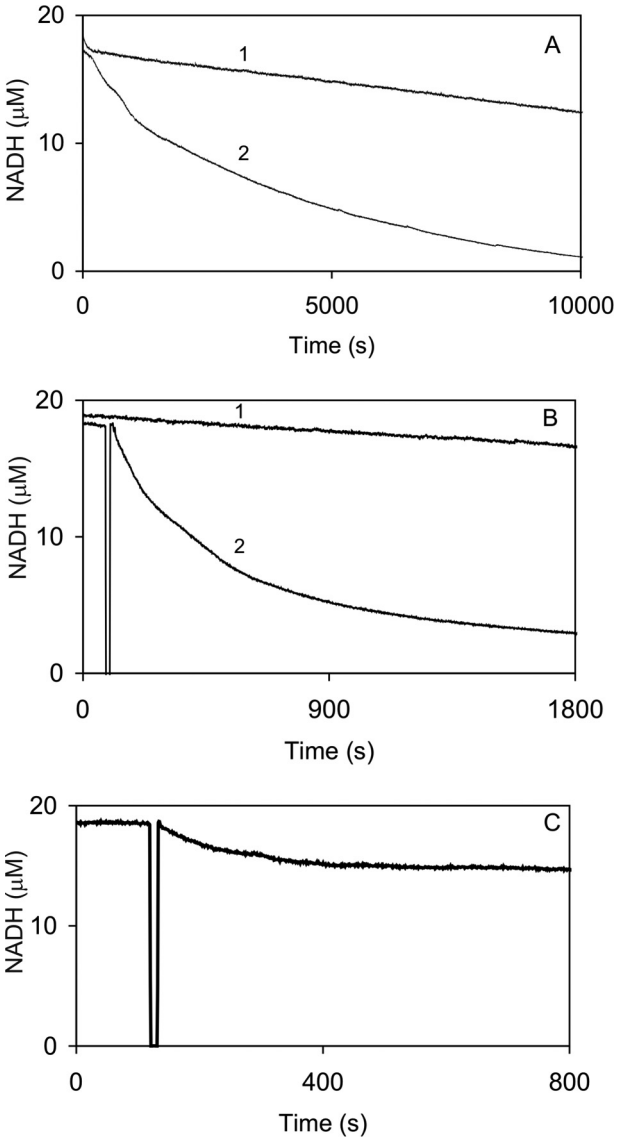

FIGURE 5. **Autoinactivation of phospho-Thr^{286}-αCaMKII in the presence of Ca^{2+}.** Temperature-dependent αCaMKII activity and time-dependent inactivation of Ca^{2+}/CaM·phospho-Thr^{286}-αCaMKII was monitored in the NADH-coupled assay. Activity of 50 nM enzyme in the presence of 50 μM syntide 2 as peptide substrate at 10 μM [Ca^{2+}] concentration was measured at 22 (*A*), 30 (*B*), and 37 °C (*C*). Exponential decays of activity (*traces 2* at 22 and 30 °C) were corrected for photobleaching (*traces 1* at 22 and 30 °C) and were fitted with rate constants.

[4] C. Fraser and K. Török, unpublished observation.

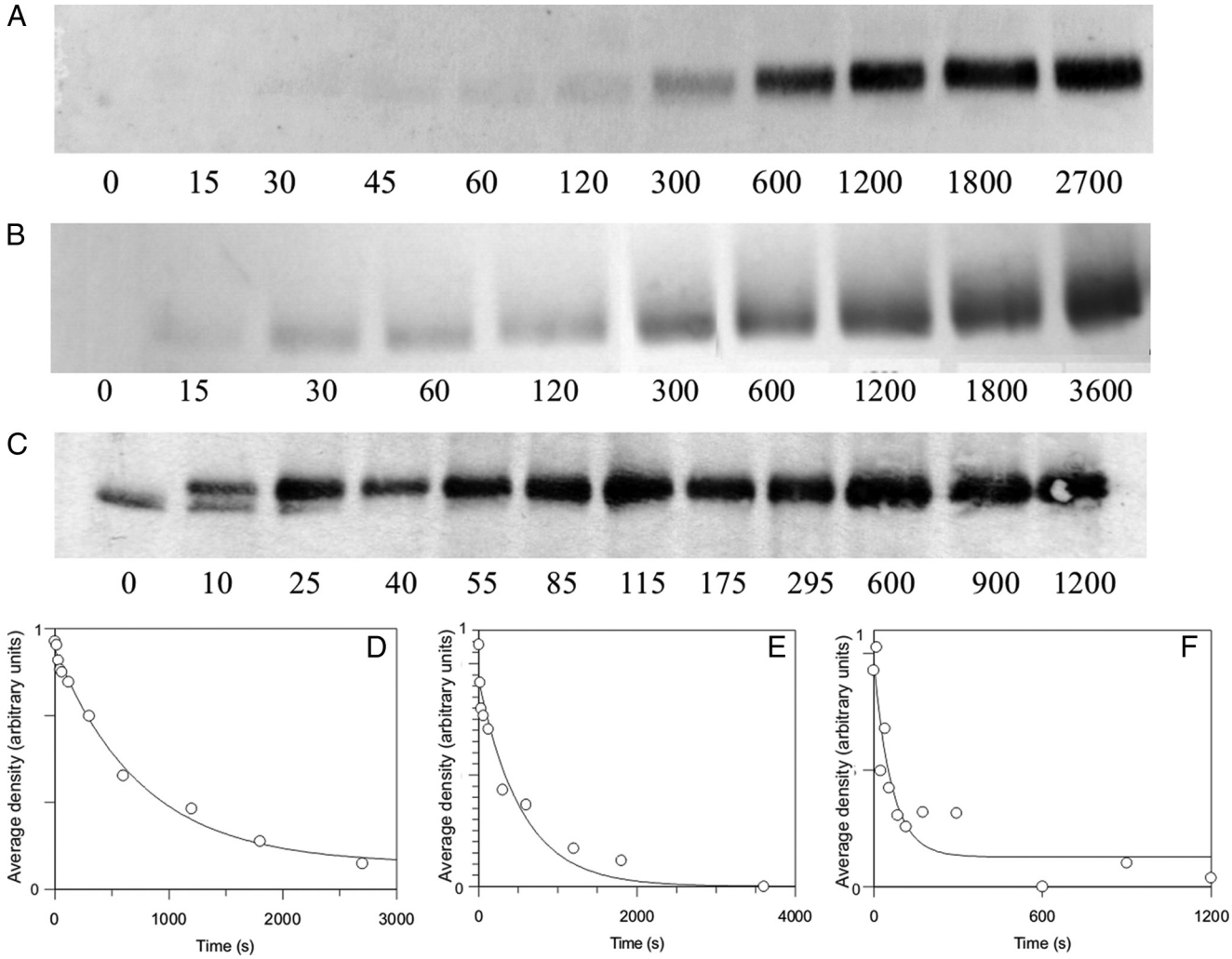

FIGURE 6. **Thr$^{305/306}$ autophosphorylation in the presence of Ca^{2+}.** Thr$^{305/306}$ autophosphorylation time course estimated by Western blotting. 1 μM αCaMKII was allowed to autophosphorylate for the indicated lengths of time as described under "Materials and Methods." Aliquots were taken at the indicated time points; the reaction was quenched by pipetting the aliquots taken into SDS sample buffer. Shown are Western blots and respective densitometric analyses of representative time courses at 21 (*A* and *D*), 30 (*B* and *E*), and 37 °C (*C* and *F*). Care was taken that the intensity of the bands was in the quasilinear range of densities (for details, see Fig. 3). Densitometric analysis of Western blots was carried out as described under "Materials and Methods."

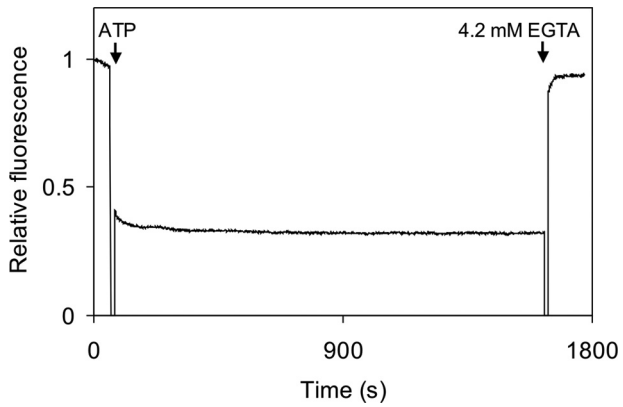

FIGURE 7. **Ca^{2+}/DA-CaM trapping in phospho-Thr^{286}-αCaMKII during Thr$^{305/306}$-autophosphorylation.** 0.5 μM DA-CaM and 1 μM αCaMKII were preincubated at 37 °C; DA-CaM fluorescence intensity was defined as 1. At the point indicated by an *arrow*, 1 mM ATP was added, resulting in substantial quenching of DA-CaM fluorescence, indicating its adopting a compact conformation bound to phospho-Thr^{286}-αCaMKII. As indicated by the *second arrow*, at 1600 s, 4.2 mM EGTA was added, resulting in unquenching of DA-CaM fluorescence, indicating the stretching of DA-CaM to an extended conformation.

seen however, that DA-CaM fluorescence remained quenched in the autoinhibited and presumed Thr$^{286/305/306}$-phosphoenzyme complex, as monitored for 4000 s at 21 °C (not shown) and 1600 s at 37 °C (Fig. 7). In the latter conditions, as shown above, autoinactivation occurred with a $t_{1/2}$ of 50 s. Ca^{2+}/DA-CaM supports both Thr^{286} and Thr$^{305/306}$ autophosphorylation (data not shown). These data show that Thr$^{305/306}$ autophosphorylation of phospho-Thr$_{286}$-αCaMKII proceeds in the presence of bound Ca^{2+}/CaM, contrary to previous reports suggesting that CaM dissociation is a prerequisite for it to occur.

Arrhenius Plots of Temperature Dependences of Activation and Autoinactivation Processes of αCaMKII—Fig. 8 shows the Arrhenius plots of the measured reactions. Data set 1 represents the temperature dependence of the turnover rate of αCaMKII-phosphorylating peptide substrate syntide-2. This reaction had a high ln *A* value and an E_a of 101 kJ/mol; these values were consistent with a favorable reaction characterized by a transition state that was more highly disordered than the ground state, an average activation energy, and a fast rate constant (14.6 s^{-1} at 37 °C). The values for data set 2 were esti-

mated using published data for the Thr^{286} autophosphorylation reaction (26). These values show a reaction similarly favorable and rapid as substrate phosphorylation, consistent with the observation that Thr^{286} autophosphorylation occurs in preference to substrate phosphorylation (Fig. 1) (27).

The autoinactivation reactions were represented by a distinctly different group of Arrhenius plots compared with those of activation. Data set 3 illustrates the inactivation induced by EGTA addition, and data set 4 corresponds to autoinactivation that occurs in the presence of Ca^{2+}, following activation and Thr^{286} autophosphorylation. The E_a value for EGTA-induced inactivation (data set 3) was 106 kJ/mol; the ln *A* value was, however, much lower than that for the activation processes. Similar values were obtained for $Thr^{305/306}$ autophosphorylation (data set 5 and Table 2), indicating an unfavorable reaction in which the transition state may be more ordered than the ground state. A low rate of reaction may thus be due to a reduction in the degrees of freedom during acquisition of the transition state. The rates and temperature dependence of autoinactivation in the presence of Ca^{2+} were similar to those in EGTA in the 30–37 °C range (data set 6). Although the inactivation rates in Ca^{2+} when fitted gave an E_a value of 172 kJ/mol, this value was not significantly different from the others for inactivation and $Thr^{305/306}$ autophosphorylation.

The temperature dependence of the reaction rates shows that distinct, less favorable structural changes underlie the autoinactivation processes compared with those for activation. Correspondingly, there is a difference of approximately 3 orders of magnitude between the activation and inactivation rates of αCaMKII. At physiological temperature (37 °C), however, the autoinactivation processes occur with a $t_{½}$ of ~1 min, which is in the range of relevant rates for signal transduction and may explain the observed inactivation in chemically induced long term potentiation (22).

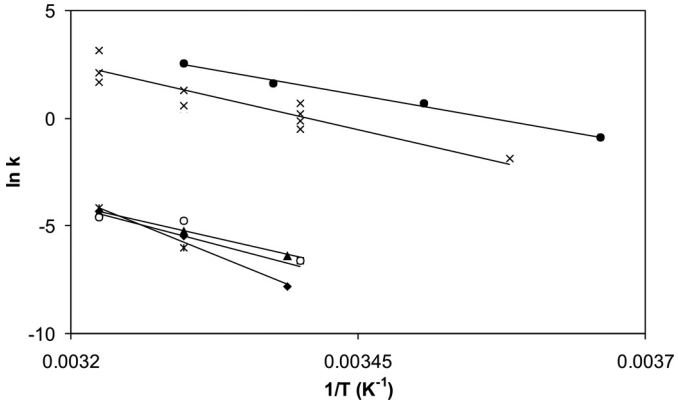

FIGURE 8. **Arrhenius plots of activation and inactivation processes of αCaMKII.** Turnover rates were calculated from steady-state activity measurements (data set 1; ●); Thr^{286} autophosphorylation rates were estimated using data from a previous publication (26) where autonomous activity was used as a measure of Thr^{286} autophosphorylation (data set 2, ×); inactivation rates were obtained in EGTA (data set 3; ▲); and Ca^{2+} (data set 4; ◆) and $Thr^{305/306}$ autophosphorylation rates were measured in EGTA (data set 5; *) and Ca^{2+} (data set 6; ○), as described above (also see Table 1).

DISCUSSION

First, the conditions of phospho-Thr^{286}-αCaMKII formation were studied. In our observation, Thr^{286} autophosphorylation and phosphorylation of an exogenous peptide substrate have similar Ca^{2+} dependences with K_m values of ~500 nM for Ca^{2+}. This value is typical for the [Ca^{2+}] responsible for activation. It is, however, at variance with the previously reported K_m or EC_{50} values for Ca^{2+} for Thr^{286} autophosphorylation of 1.6 μM (26) and 2 μM (28), obtained by the measurement of "autonomous" activity and Thr^{286} autophosphorylation by Western blotting, respectively. An *n* value of ~8 for Ca^{2+} activation was measured, suggesting that the Ca^{2+} sites from two CaM molecules are simultaneously involved, supporting the previously determined intersubunit mechanism for Thr^{286} autophosphorylation (29). Such a high *n* value has previously been reported for the measurement of "autonomous" activity in the presence of phosphatase only (26). These discrepancies are probably related to "autonomous" activity measurements being greatly dependent on experimental conditions. Our data furthermore clearly show that Thr^{286} autophosphorylation occurs immediately upon activation and that it proceeds regardless of the presence of saturating exogenous peptide substrate, demonstrating the highly preferential nature of Thr^{286} autophosphorylation over an exogenous substrate (27).

Autoinactivation of phospho-Thr^{286}-αCaMKII was investigated in two different conditions. Ca^{2+} sequestration and Ca^{2+}-induced autoinactivation had common and distinct features; both were characterized by $Thr^{305/306}$ autophosphorylation, but the fate of CaM was distinct. Upon Ca^{2+} sequestration, Ca^{2+}/CaM sequential lobe dissociation occurred, whereas in the presence of Ca^{2+}, Ca^{2+}/CaM remained trapped in phospho-Thr^{286}-αCaMKII during $Thr^{305/306}$ autophosphorylation and autoinactivation.

In the mechanism of inactivation upon Ca^{2+} sequestration following initial activation by Ca^{2+}/CaM, one CaM lobe was shown to dissociate rapidly, but the second lobe remained attached, probably by virtue of a high affinity Ca^{2+} binding site in trapped CaM (19). The structures of the Ca^{2+}/CaM·peptide complexes of peptides derived from the CaM binding domain of αCaMKII show anti-parallel binding (30), suggesting that the N lobe of CaM is attached to the C-terminal region of the CaM binding domain in the proximity of or over the $Thr^{305/306}$ sites. Thus, according to previous models, dissociation of the N lobe,

TABLE 2

Arrhenius parameters of activity, autophosphorylation, and inactivation of the Ca^{2+}/CaM·phospho-Thr^{286}-αCaMKII complex

Arrhenius plots were constructed from temperature-dependent activation and inactivation data sets obtained in the specified conditions. Each set of data was fitted by linear regression.

Activity		Thr^{286} autophosphorylation		Inactivation (EGTA)		Thr^{305} autophosphorylation (EGTA)		Inactivation (Ca^{2+})		Thr^{305} autophosphorylation (Ca^{2+})	
E	ln *A*	*E*	ln *A*	*E*	ln *A*	*E*	ln *A*	*E*	ln *A*	*E*	ln *A*
kJ/mol		*kJ/mol*		*kJ/mol*		*kJ/mol*		*kJ/mol*		*kJ/mol*	
101	41.4	77	33.10	106	36.7	99	34.1	172	62.5	114	39.9

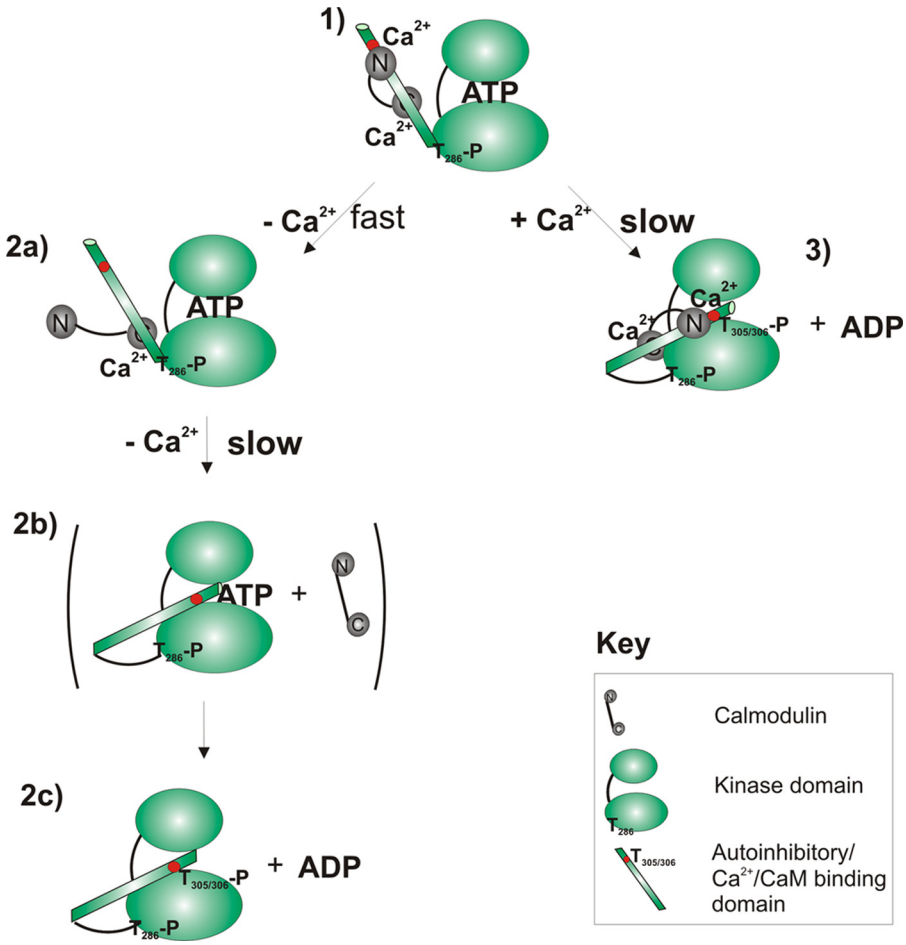

SCHEME 1. **Mechanisms of auto-inactivation of Ca^{2+}/CaM·phospho-Thr^{286}-αCaMKII.** Two alternative pathways of autoinactivation leading to $Thr^{305/306}$ autophosphorylation are illustrated from the perspective of a single kinase domain. The *top* and *bottom ellipses* represent the β-sheeted propeller domain and the α-helical substrate binding domain connected by a hinge and with the ATP binding site in between (4). The pathway in the *left column* includes initial rapid dissociation of the CaM N lobe followed by a slow conformational change accompanying the dissociation of the CaM C lobe, allowing a conformational change permissive for $Thr^{305/306}$ autophosphorylation to occur. This path results in an inactivated enzyme complex free of CaM. *1*, active Ca^{2+}/CaM·phospho-Thr^{286}-αCaMKII; the autoinhibitory domain is detached from the kinase domain and is Ca^{2+}/CaM-bound. *2*, upon Ca^{2+} chelation by EGTA, rapid dissociation of the N lobe of CaM is seen. *2b*, slow dissociation of CaM C lobe; slow conformational change positions $Thr^{305/306}$ as a "canonical" substrate, adjacent to the ATP binding pocket. *2c*, $Thr^{305/306}$ autophosphorylation of Ca^{2+}/CaM-free kinase. In the *right-hand column*, $Thr^{305/306}$ autophosphorylation of the Ca^{2+}/CaM-bound phospho-Thr^{286}-αCaMKII is shown. *3*, slow conformational change leads to the conformation permissible for $Thr^{305/306}$-autophosphorylation.

which is likely to correspond to the rapid phase of CaM dissociation, should allow $Thr^{305/306}$ autophosphorylation. If N lobe dissociation controlled $Thr^{305/306}$ autophosphorylation, it would thus be rapid (31). However, this was not seen. $Thr^{305/306}$ autophosphorylation correlated with the slow phase of dissociation, assumed to represent the C lobe (Scheme 1). Thus, our data show that exposure of the $Thr^{305/306}$ residues is not sufficient to allow their autophosphorylation.

Is complete dissociation of CaM required for $Thr^{305/306}$ autophosphorylation? $Thr^{305/306}$ autophosphorylation is shown here to proceed in the continued presence of Ca^{2+} with rates similar to those in its absence. $Thr^{305/306}$ autophosphorylation observed in the presence of Ca^{2+} was expected to occur with the concomitant dissociation of at least the CaM lobe that binds at or near residues $Thr^{305/306}$. Our DA-CaM experiments, however, showed no detectable change in the compact structure of Ca^{2+}/CaM, indicating that Ca^{2+}/CaM remained bound throughout the experiment, ~30 min at 37 °C. Despite predictions, Ca^{2+}/CaM dissociation was not required for $Thr^{305/306}$ autophosphorylation to occur. Interestingly, the rate of $Thr^{305/306}$ autophosphorylation resembled that of Ca^{2+}/CaM dissociation in Ca^{2+} (17), suggesting that CaM binding dynamics may play a role.

Since autoinactivation is contemporaneous with the slow dissociation of the second CaM lobe, it is further evident that rapid dissociation of the presumed N lobe of CaM does not cause inhibition of phospho-Thr^{286}-αCaMKII. It is important to consider whether the state in which phospho-Thr^{286}-αCaMKII has CaM attached by one lobe only (presumed to be the C lobe) has any special properties in terms of activity and if it limits the rate of $Thr^{305/306}$ autophosphorylation. Although the existence of stable, partially Ca^{2+}-saturated CaM-bound phospho-Thr^{286}-αCaMKII has been demonstrated at Ca^{2+} concentrations that correspond to resting intracellular [Ca^{2+}] (19), further work is required to establish their functional significance.

How does autonomous activity fit into the observed processes? Interestingly, whether autonomy is considered during Ca^{2+} sequestration or in the continuous presence of Ca^{2+}, it is difficult to find a time window for such a process. The enzyme is not inactive until both CaM lobes have dissociated; thus, C lobe-attached partially Ca^{2+}-saturated CaM may be the active species. Upon Ca^{2+} dissociation from the high affinity Ca^{2+} site and the subsequent dissociation of the second CaM lobe, inactivation occurs, and thus there appears to be no time window for autonomous activity.

The activity of Ca^{2+}/CaM-bound phospho-Thr^{286}-αCaMKII also declines in time. It is unclear at present by what mechanism phospho-Thr^{286}-αCaMKII becomes inactivated upon the continued presence of Ca^{2+}/CaM. Inactivation in the presence of Ca^{2+} has been shown to occur by self-association (32). Autoinactivation in Ca^{2+} observed here, however, does not appear to be the same process as self-association, which was seen at 10 μM ATP and pH 6.3 (32). Our experimental conditions of 1 mM ATP and pH 7.0 would not be expected to give rise to self-association.

As seen in the Arrhenius plots, the rates of autoinactivation correlated well with those of $Thr^{305/306}$ autophosphorylation.

This suggests that similar intermediates and mechanisms may lead up to $Thr^{305/306}$ autophosphorylation and autoinactivation irrespective of the presence or absence of bound Ca^{2+}/CaM. It is worth noting that the existence of phospho-$Thr^{286/305/306}$-αCaMKII itself has not been directly confirmed, since detection of autophosphorylation by immunotechniques does not allow definitive determination of whether the same subunit of αCaMKII becomes autophosphorylated in all three sites. If phospho-$Thr^{286/305/306}$-αCaMKII can be reactivated by selective dephosphorylation at $Thr^{305/306}$, the Ca^{2+}/CaM-bound and free forms may have different susceptibilities to phosphatases (33, 34).

The NR2B subunit of the NMDA receptor has been reported to fix αCaMKII in an active state (35). It has, however, also been shown that the resulting activity is very low compared with that with other substrates (11), that NR2B in fact is an effective noncompetitive inhibitor of αCaMKII activity (10), and that it does not prevent $Thr^{305/306}$ autophosphorylation (10) and is thus unlikely to prevent the above described autoinhibition.

It is concluded that Ca^{2+}/CaM binding does not determine the rate of $Thr^{305/306}$ autophosphorylation but that slow conformational changes in the phospho-Thr^{286}-αCaMKII enzyme result in a conformation permissible to $Thr^{305/306}$-autophosphorylation with or without Ca^{2+} and CaM present. $Thr^{305/306}$ autophosphorylation may be the common process that is responsible for autoinhibition both in the presence and absence of Ca^{2+} (Scheme 1). Further questions do, however, still remain as to by what mechanism $Thr^{305/306}$ autophosphorylation may cause inactivation.

In conclusion, phospho-Thr^{286}-αCaMKII, universally the functionally essential form of αCaMKII, appears to be programmed for autoinactivation, having a brief time window of ~1 min to exert its activity. After this, new enzyme is required to respond to new Ca^{2+} stimuli. These observations suggest a transient activity by αCaMKII at the synapse and may explain why new protein synthesis is required from local mRNA in synaptic plasticity (36). Coincidentally, transient activation of αCaMKII in single dendritic spines lasting for ~1 min has been reported during long term potentiation; however, the mechanism of inactivation has yet to be determined *in vivo* (34).

REFERENCES

1. Fukunaga, K., and Miyamoto, E. (1999) *Jpn. J. Pharmacol.* **79,** 7–15
2. Nicoll, R. A., and Malenka, R. C. (1999) *Ann. N.Y. Acad. Sci.* **868,** 515–525
3. Schulman, H., and Lou, L. L. (1989) *Trends Biochem. Sci.* **14,** 62–66
4. Johnson, L. N. (2001) *Ernst Schering Res. Found. Workshop* **34,** 47–69
5. Wang, Z. W. (2008) *Mol. Neurobiol.* **38,** 153–166
6. Barria, A., Muller, D., Derkach, V., Griffith, L. C., and Soderling, T. R. (1997) *Science* **276,** 2042–2045
7. Hashimoto, Y., and Soderling, T. R. (1987) *Arch. Biochem. Biophys.* **252,** 418–425
8. Morris, E. P., and Török, K. (2001) *J. Mol. Biol.* **308,** 1–8
9. Miller, S. G., and Kennedy, M. B. (1986) *Cell* **44,** 861–870
10. Robison, A. J., Bartlett, R. K., Bass, M. A., and Colbran, R. J. (2005) *J. Biol. Chem.* **280,** 39316–39323
11. Pradeep, K. K., Cheriyan, J., Suma Priya, S. D., Rajeevkumar, R., Mayadevi, M., Praseeda, M., and Omkumar, R. V. (2009) *Biochem. J.* **419,** 123–132
12. Ishida, A., and Fujisawa, H. (1995) *J. Biol. Chem.* **270,** 2163–2170
13. Strack, S., and Colbran, R. J. (1998) *J. Biol. Chem.* **273,** 20689–20692
14. Ishida, A., Kitani, T., and Fujisawa, H. (1996) *Biochim. Biophys. Acta* **1311,** 211–217
15. Tzortzopoulos, A., and Török, K. (2004) *Biochemistry* **43,** 6404–6414
16. Meyer, T., Hanson, P. I., Stryer, L., and Schulman, H. (1992) *Science* **256,** 1199–1202
17. Török, K., Tzortzopoulos, A., Grabarek, Z., Best, S. L., and Thorogate, R. (2001) *Biochemistry* **40,** 14878–14890
18. Tse, J. K., Giannetti, A. M., and Bradshaw, J. M. (2007) *Biochemistry* **46,** 4017–4027
19. Tzortzopoulos, A., Best, S. L., Kalamida, D., and Török, K. (2004) *Biochemistry* **43,** 6270–6280
20. Lisman, J., Schulman, H., and Cline, H. (2002) *Nat. Rev. Neurosci.* **3,** 175–190
21. Wang, H., Feng, R., Phillip Wang, L., Li, F., Cao, X., and Tsien, J. Z. (2008) *Curr. Biol.* **18,** 1546–1554
22. Lengyel, I., Voss, K., Cammarota, M., Bradshaw, K., Brent, V., Murphy, K. P., Giese, K. P., Rostas, J. A., and Bliss, T. V. (2004) *Eur. J. Neurosci.* **20,** 3063–3072
23. Hashimoto, Y., Schworer, C. M., Colbran, R. J., and Soderling, T. R. (1987) *J. Biol. Chem.* **262,** 8051–8055
24. Török, K., Wilding, M., Groigno, L., Patel, R., and Whitaker, M. (1998) *Curr. Biol.* **8,** 692–699
25. Smith, G. L., and Miller, D. J. (1985) *Biochim. Biophys. Acta* **839,** 287–299
26. Bradshaw, J. M., Kubota, Y., Meyer, T., and Schulman, H. (2003) *Proc. Natl. Acad. Sci. U.S.A.* **100,** 10512–10517
27. Grant, P. A., Best, S. L., Sanmugalingam, N., Alessio, R., Jama, A. M., and Török, K. (2008) *Cell Calcium* **44,** 465–478
28. Shifman, J. M., Choi, M. H., Mihalas, S., Mayo, S. L., and Kennedy, M. B. (2006) *Proc. Natl. Acad. Sci. U.S.A.* **103,** 13968–13973
29. Hanson, P. I., Meyer, T., Stryer, L., and Schulman, H. (1994) *Neuron* **12,** 943–956
30. Meador, W. E., Means, A. R., and Quiocho, F. A. (1992) *Science* **257,** 1251–1255
31. Mukherji, S., and Soderling, T. R. (1995) *J. Biol. Chem.* **270,** 14062–14067
32. Hudmon, A., Aronowski, J., Kolb, S. J., and Waxham, M. N. (1996) *J. Biol. Chem.* **271,** 8800–8808
33. Strack, S., Barban, M. A., Wadzinski, B. E., and Colbran, R. J. (1997) *J. Neurochem.* **68,** 2119–2128
34. Lee, S. J., Escobedo-Lozoya, Y., Szatmari, E. M., and Yasuda, R. (2009) *Nature* **458,** 299–304
35. Bayer, K. U., De Koninck, P., Leonard, A. S., Hell, J. W., and Schulman, H. (2001) *Nature* **411,** 801–805
36. Roberts, L. A., Large, C. H., Higgins, M. J., Stone, T. W., O'Shaughnessy, C. T., and Morris, B. J. (1998) *Brain Res. Mol. Brain Res.* **56,** 38–44